JASA Express Letters

OCTOBER 11 2023

Computation of spherical sector harmonics norm with application to blind source separation

Deepika Kumari ; Lalan Kumar

JASA Express Lett. 3, 104801 (2023)
https://doi.org/10.1121/10.0021316

JASA EXPRESS LETTERS ARTICLE asa.scitation.org/journal/jel

Computation of spherical sector harmonics norm with application to blind source separation

Deepika Kumari[1] and Lalan Kumar[2,a)]
[1]Department of Electrical Engineering, Indian Institute of Technology, Delhi 110016, India
[2]Department of Electrical Engineering and Bharti School of Telecommunication, Indian Institute of Technology, Delhi 110016, India
deepikakumari.ee@gmail.com, lkumar@ee.iitd.ac.in

Abstract: Spherical microphone arrays (SMAs) are widely being used for source localization and separation. However, it is uneconomical to build a full SMA when sources are present in restricted regions of environment. Hence, a spherical sector microphone array is utilized for blind source separation for the first time. In particular, the norm of the spherical sector harmonics basis function is computed for mixing matrix estimation. The estimated steering vectors are clustered using mean-shift algorithm. The number of sources is estimated automatically from the number of clusters. The developed mathematical framework is verified using various simulations and experiments on real data.

[Editor: David C Swanson] https://doi.org/10.1121/10.0021316

Received: 17 May 2023 **Accepted:** 19 September 2023 **Published Online:** 11 October 2023

1. Introduction

Spherical harmonics (SH) domain signal processing utilizing a spherical microphone array (SMA) has received much attention in recent years. This is because of the ease of array processing in the SH domain with no spatial ambiguity. Hence, the SMA has widely been used for acoustic source localization,[1] imaging,[2] and source separation.[3]

However, building an SMA over a rigid sphere is a challenging task. Additionally, using the complete sphere involves more microphones and information to process. It is also uneconomic to use SMA when sources are present in restricted regions of the environment. As a result, a recent trend has emerged for the use of a microphone array over spherical sector. Li *et al.* utilized a hemispherical microphone array (HMA) for sound acquisition and beamforming.[4] Acoustic image principle (AIP) was utilized therein, facilitating the use of SH, an orthonormal basis function defined over the sphere. Hemispherical harmonics (HSH),[5] an orthonormal basis function defined over HMA, was utilized for sound source localization.[6] A microphone array placed over one-eighth, quarter, and half-spaces was utilized for beamforming.[7] Spherical fraction harmonics were utilized therein. Orthonormal spherical sector harmonics (S^2H) basis functions over a general spherical sector microphone array were derived for sound-field representation[8] and were utilized for subsequent localization.[9]

Blind source separation (BSS) is used to extract source signals that are mixed by an unknown medium and delivered by an array of sensors. It has extensive application in communications, speech, and biomedical signals processing.[10,11] There have been different approaches to blind source separation that include learning based[12] and statistical based.[13] Independent component analysis (ICA) for BSS exploits statistical independence and non-Gaussianity of the mixture components.[14] The joint approximate diagonalization of eigenmatrices (JADE) algorithm has been utilized for BSS.[15] BSS for time-frequency (t-f) overlapped sources in anechoic environment, was used by Aissa-El-Be *et al.*[16] However, it assumes that the number of sources is known. The estimation of mixing matrix with unknown number of sources in short-time Fourier transform (STFT) domain was presented by Zhang *et al.*[17] A clustering based approach to BSS was used by He *et al.*[18] The method uses the learning algorithm to estimate the mixing matrix. The numerical performance criteria is designed to evaluate the BSS algorithm.[19] A standard linear ICA model was utilized for higher-order ambisonic (HOA) domain based blind separation of convolutive mixtures using SMA.[3]

In this paper, blind source separation using a spherical sector array is attempted for the first time. In particular, a spherical sector harmonics clustering based approach is adopted.

2. Spherical sector harmonics norm

A spherical sector microphone array of order N, radius r, and the number of sensors I is considered. The sector is, in general, defined by elevation $[\theta_1, \theta_2]$ and azimuth $[\phi_1, \phi_2]$. For the plausible solution to wave equation over the sector, ϕ_1 is

a)Author to whom correspondence should be addressed.

taken to be zero with $\phi_2 = 2\pi/u$, where $u \geq 1$.[8] A sound field of L plane-waves with wave number k is incident on the array. The lth source location is denoted by $\Psi_l = (\theta_l, \phi_l)$, where θ is the elevation angle and ϕ is azimuth angle. The ith sensor location is given by $\mathbf{r_i} = (r, \Phi_i)^T$, where $\Phi_i = (\theta_i, \phi_i)$ and $(\cdot)^T$ is the transpose of $(\cdot)$.

2.1 Array data model in S^2H-STFT domain

The source separation is performed using discrete time-frequency signal $\mathbf{P}(\tau, \nu)$, given by[9]

$$\mathbf{P}(\tau, \nu) = \mathbf{A}(k)\mathbf{S}(\tau, \nu) + \mathbf{N}(\tau, \nu), \tag{1}$$

where $\mathbf{A}(k)$, $\mathbf{S}(\tau, \nu)$, and $\mathbf{N}(\tau, \nu)$ are the steering, signal, and noise matrices, respectively. τ is the time frame index and ν is frequency bin index. The wave number k is related to the frequency bin index ν as $k = 2\pi f/c = 2\pi\nu f_s/(cW)$. Here, f_s is the sampling frequency, f is the continuous frequency, c is the speed of sound, and W is the window length. The spherical sector harmonics (S^2H) decomposition (S^2HD) of the received pressure in Eq. (1) is given as[9]

$$\begin{aligned}\mathbf{P}_{nm}(\tau, \nu) &= \int_{\phi_1}^{\phi_2}\int_{\theta_1}^{\theta_2} \mathbf{P}(\tau, \nu)\left[T_n^m(\Phi)\right]^* \sin(\theta) d\theta d\phi \\ &\cong \sum_{i=1}^{I} \alpha_i \mathbf{P_i}(\tau, \nu)\left[T_n^m(\Phi_i)\right]^*,\end{aligned} \tag{2}$$

where α_i is the sampling weight of the ith sensor,[20] $(\cdot)^*$ is complex conjugate of $(\cdot)$, and $T_n^m(\Phi_i)$ represents the S^2H basis function of order n and degree m, given by[9]

$$T_n^m(\Phi_i) = \begin{cases} K_n^m \tilde{\mathcal{P}}_n^m(\cos\theta_i)\tilde{e}^{jm\phi_i} & \forall\, 0 \leq n \leq \infty, 0 \leq m \leq n, \\ (-1)^{|m|} T_n^{|m|*}(\Phi_i) & \forall\, -n \leq m < 0, \end{cases} \tag{3}$$

where $\tilde{\mathcal{P}}_n^m(\cos\theta_i)$ is the shifted associated Legendre polynomials. The spatial steering matrix in Eq. (1) can be re-written using S^2H as[9]

$$\mathbf{A}(k) = \mathbf{T}(\Phi)\mathbf{B}(kr)\mathbf{T}^H(\Psi). \tag{4}$$

The details of normalization constant K_n^m and mode strength matrix $\mathbf{B}(kr)$ is presented by Kumari *et al.*[9] $\mathbf{T}(\Psi)$ is an $L \times (N+1)^2$ matrix whose lth row is

$$\mathbf{t}(\Psi_l) = \left[\, T_0^0(\Psi_l), \quad T_1^{-1}(\Psi_l), \quad T_1^0(\Psi_l), \quad \ldots, \quad T_N^N(\Psi_l) \,\right]. \tag{5}$$

Re-writing Eq. (2) in a matrix form, we have

$$\mathbf{P_{nm}}(\tau, \nu) \cong \mathbf{T}^H(\Phi)\mathbf{\Gamma}\mathbf{P}(\tau, \nu), \tag{6}$$

where $\mathbf{\Gamma} = \mathrm{diag}(\alpha_1, \alpha_2, \ldots, \alpha_I)$. Substituting Eq. (4) in Eq. (1), multiplying both sides with $\mathbf{T}^H(\Phi)\mathbf{\Gamma}$ and then utilizing $\mathbf{T}^H(\Phi)\mathbf{\Gamma}\mathbf{T}(\Phi) \approx \mathbf{I}$ and Eq. (6), we have

$$\mathbf{P_{nm}}(\tau, \nu) = \mathbf{B}(kr)\mathbf{T}^H(\Psi)\mathbf{S}(\tau, \nu) + \mathbf{N_{nm}}(\tau, \nu). \tag{7}$$

As the mode strength is constant for a particular array configuration, the plane wave decomposition (PWD) is obtained by multiplying both sides of Eq. (7) with $\mathbf{B}^{-1}(kr)$. This results in the final S^2H-STFT data model, given by

$$\mathbf{D_{nm}}(\tau, \nu) = \mathbf{T}^H(\Psi)\mathbf{S}(\tau, \nu) + \mathbf{Z_{nm}}(\tau, \nu), \tag{8}$$

where $\mathbf{D_{nm}}(\tau, \nu) = \mathbf{B}^{-1}(kr)\mathbf{P_{nm}}(\tau, \nu)$ and $\mathbf{Z_{nm}}(\tau, \nu) = \mathbf{B}^{-1}(kr)\mathbf{N_{nm}}(\tau, \nu)$. $\mathbf{T}^H(\Psi)$ is the new steering matrix in S^2H-STFT domain.

2.2 Computation of S^2H norms

S^2H norm for clustering based blind source separation (BSS) is computed in this section. The square of L2 norm of $\mathbf{t}^H(\Psi_l)$ can be written using Eq. (5) as

$$||\mathbf{t}^H(\Psi_l)||^2 = \sum_{n=0}^{N}\sum_{m=-n}^{n}\left[T_n^m(\Psi_l)\right]^* T_n^m(\Psi_l). \tag{9}$$

The S^2H addition theorem is given by[8]

$$\sum_{m=-n}^{n}\left[T_n^m(\Psi_l)\right]^* T_n^m(\Phi_i) = \frac{(2n+1)q_1 * u}{4\pi}\mathcal{P}_n(q_1\cos\gamma + q_2), \tag{10}$$

where γ denotes the angle between Ψ_l and Φ_i and (q_1, q_2, u) defines the elevation and azimuth range for the sector. Utilizing the addition theorem of S^2H with $\gamma = 0$, Eq. (9) can be simplified as

$$||\mathbf{t}^H(\Psi_l)||^2 = \sum_{n=0}^{N} \frac{(2n+1)q_1 u}{4\pi} \mathcal{P}_n(q_1+q_2). \tag{11}$$

For a spherical sector with $\theta \in [0°,90°]$, and $\phi \in [0°,360°]$, the parameters of the S^2H are calculated as $q_1 = 2$, $q_2 = -1$, and $u = 1$. Utilizing these values along with $\mathcal{P}_n(1) = 1$ in Eq. (11) gives

$$||\mathbf{t}^H(\Psi_l)||^2 = \frac{2}{4\pi} \sum_{n=0}^{N} (2n+1). \tag{12}$$

Upon simplifying, the final S^2H norms for the given sector can be written as

$$||\mathbf{t}^H(\Psi_l)|| = \frac{(N+1)}{\sqrt{2\pi}}. \tag{13}$$

3. Application to blind source separation

In this section, S^2H norm is utilized for clustering based blind source separation (BSS). The BSS problem is addressed herein with unknown number of sources. The data model in Eq. (8) is utilized for this purpose. We need to first estimate the number of sources and then the mixing matrix. The mixing matrix will be utilized thereafter for BSS. Re-writing the linear time-frequency data model from Eq. (8) we have

$$\mathbf{D_{nm}}(\tau,\nu) = \mathbf{T}^H(\Psi)\mathbf{S}(\tau,\nu) + \mathbf{Z_{nm}}(\tau,\nu), \quad (\tau,\nu) \in \Omega_0, \tag{14}$$

where Ω_0 is the set including all the (τ,ν) points in STFT domain. Noise thresholding is applied to remove the noisy t-f points. If for any t-f point

$$\frac{||\mathbf{D_{nm}}(\tau,\nu)||}{\max||\mathbf{D_{nm}}(\tau,\nu)||} > \epsilon, \tag{15}$$

the t-f point is retained where ϵ is a small threshold, typically 0.02. Such t-f points form new set Ω. For noiseless case, the data model in Eq. (14) can be written as

$$\mathbf{D_{nm}}(\tau,\nu) = \mathbf{T}^H(\Psi)\mathbf{S}(\tau,\nu), \quad (\tau,\nu) \in \Omega. \tag{16}$$

Under the assumption of disjoint sources in the t-f domain, the data model in Eq. (16) can be simplified as

$$\mathbf{D_{nm}}(\tau_a,\nu_a) = \mathbf{t}^H(\Psi_l)\mathbf{S}_l(\tau_a,\nu_a), \tag{17}$$

where $(\tau_a,\nu_a) \in \Omega_l$ and $\Omega = \cup_{l=1}^{L}\Omega_l$. The steering vector, $\mathbf{t}^H(\Psi_l)$ for the lth source can now be estimated as

$$\frac{\mathbf{D_{nm}}(\tau_a,\nu_a)}{||\mathbf{D_{nm}}(\tau_a,\nu_a)||} = \frac{\mathbf{t}^H(\Psi_l)\mathbf{S}_l(\tau_a,\nu_a)}{||\mathbf{t}^H(\Psi_l)\mathbf{S}_l(\tau_a,\nu_a)||} = \frac{\mathbf{t}^H(\Psi_l)}{||\mathbf{t}^H(\Psi_l)||}. \tag{18}$$

Utilizing Eq. (13), the steering vector can be estimated as

$$\hat{\mathbf{t}}^H(\Psi_l) = \left[\frac{\mathbf{D_{nm}}(\tau_a,\nu_a)}{||\mathbf{D_{nm}}(\tau_a,\nu_a)||} \times \frac{N+1}{\sqrt{2\pi}}\right]. \tag{19}$$

The estimated steering vectors are clustered using a mean-shift algorithm.[21] The number of sources present are estimated automatically based on the number of clusters. The mean-shift algorithm utilized herein does not consider the poorly populated clusters of steering vectors resulting due to noise and overlapped t-f points. The mean-shift algorithm works on the basis of finding the densest region. It does not require the knowledge of number of clusters as in the k-means clustering

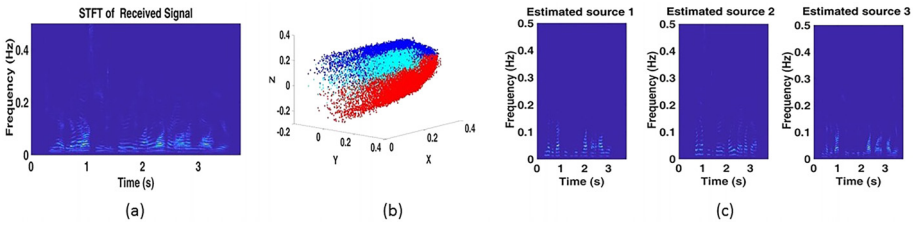

Fig. 1. Illustration of spherical sector harmonics clustering based blind source separation. (a) The STFT plot of the received mixture from one channel. (b) Three clusters of steering vectors corresponding to three sources. (c) The STFT plot of the separated sources.

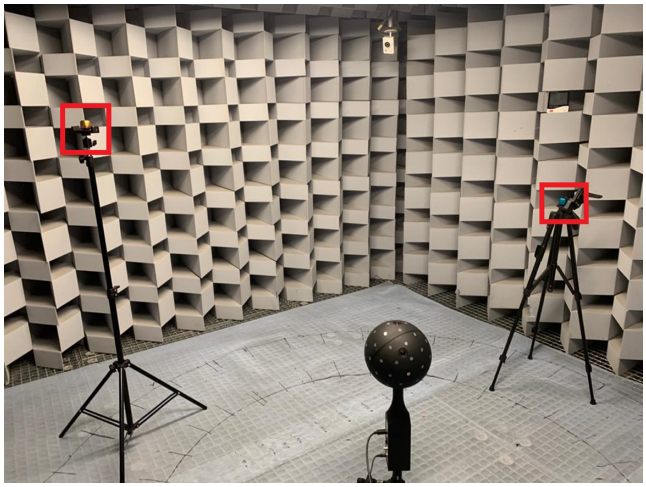

Fig. 2. Experimental setup in an anechoic chamber at IIT Delhi.

algorithm. The lth estimated steering vector, $\hat{\mathbf{t}}(\Psi_l)$ is finally given by the lth cluster center. The STFT of each source $\mathbf{S}_l(\tau_a, \nu_a)$ can now be computed as

$$\hat{\mathbf{S}}_l(\tau_a, \nu_a) \approx \hat{\mathbf{t}}(\Psi_l)\mathbf{D}_{\mathbf{nm}}(\tau_a, \nu_a). \tag{20}$$

The proposed spherical sector harmonics clustering based BSS method is illustrated in Fig. 1. Simulations are performed assuming a rigid spherical sector with $\theta \in [0°,90°]$, $\phi \in [0°,360°]$ and radius 10 cm under free-field assumption. The sector utilizes all the 30 microphones in VisiSonics system[22] with entire azimuth and $\theta \in [0°,90°]$. The selection of the spherical sector is done considering ease of installation and applications. Three speech signals from TIMIT database[23] were utilized for the simulation. The mixed signal was received over the sector from three sources with locations (30°,15°), (60°,30°), and (45°,45°) at SNR 25 dB. The array order was taken to be 4. The STFT plot for the received signal from first channel is given in Fig. 1(a). The clusters of steering vectors are plotted in Fig. 1(b). Three distinct clusters can be observed corresponding to the three sources. The centers of these clusters are the final estimated steering vectors corresponding to the sources. The estimated steering vectors are utilized for the desired source separation. The STFT plot for the separated sources is shown in Fig. 1(c).

4. Performance evaluation

Simulation and real data experiments on source separation were carried out to evaluate the proposed BSS method. Both the simulation and real data experiments utilized 30 microphones of VisiSonics SMA[22] falling over the sector with $\theta \in [0°,90°]$, and $\phi \in [0°,360°]$. The azimuth and elevation range correspond to a hemisphere. Hence, S^2H becomes identical to that of hemispherical basis.[9] The radius of SMA is 10 cm. The experimental setup for real data recording in anechoic chamber is shown in Fig. 2. The mixed signal for simulation experiments was received over the sector from two sources with locations (30°,15°) and (60°,45°). The array order was fixed as 4. Simulation experiments were carried out using 160 (80 for source 1 and 80 for source 2) sentences from the TIMIT database. Various performance metrics are presented to evaluate the proposed method.

4.1 Simulation experiments

In this section, the proposed method is verified using composite and objective measures on simulated data.

Table 1. The composite measures of the JADE, spatial clustering, SH, and proposed S^2H clustering methods at SNR 15 dB.

	JADE		Spatial clustering		SH clustering		S^2H clustering	
Measure	S1	S2	S1	S2	S1	S2	S1	S2
C_T	−0.383	1.2833	1.6049	1.8694	1.6869	1.9738	1.7468	1.9959
C_{NT}	1.4825	1.4754	2.1837	1.9687	2.2466	2.0484	2.2923	2.0820
C_{OVL}	0.4639	1.2393	1.4883	1.5234	1.5069	1.5920	1.5408	1.5979

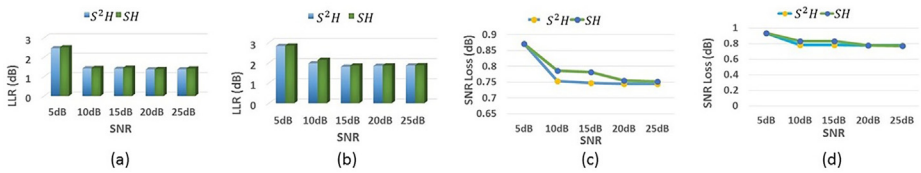

Fig. 3. The LLR and SNR Loss of the two estimated sources at (30°,15°) and (60°,45°) for various SNRs, (a), (b) LLR for estimated sources 1 and 2, respectively, and (c), (d) SNR Loss for estimated sources 1 and 2, respectively.

4.1.1 Composite measures

To estimate the quality of separated speech, composite measures denoted by C_T for target distortion, C_{NT} for non-target distortion, C_{OVL} for overall quality are utilized.[24] The composite measures are presented in Table 1 at SNR 15 dB. It is noted that the proposed S^2H based method gives better performance with higher value of C_T, C_{NT}, and C_{OVL} when compared with SH algorithm. Poor estimation in case of SH clustering method may be attributed to approximation of the function over sector using SH. Additionally, it may be observed that the source separation in SH and S^2H domains are better when compared to the spatial domain processing. Clustering based approach outperforms the JADE algorithm that additionally assumes the number of sources to be known.

4.1.2 Objective measures

Here, variation of objective measures for SH and S^2H clustering based BSS with varying SNR is presented. In particular, log likelihood ratio (LLR) and SNR loss measures are utilized. Low LLR and SNR loss indicate better separation. The objective measures are plotted in Fig. 3. It is noted that the S^2H clustering based source separation outperforms the SH algorithm for both the objective measures.

4.2 Real data experiments

The proposed S^2H clustering based method is also verified on real data. Keeping all the experimental conditions the same as detailed in Sec. 4.1, an anechoic chamber is utilized to conduct the experiment. The details of the experimental setup are shown in Fig. 2. Two mini bluetooth speakers by JBL are utilized as acoustic sources. The sources are placed at (70°,10°) and (55°,130°) in the far-field region. The clusters of steering vectors are plotted in Fig. 4(a). Two distinct clusters can be observed corresponding to the two sources. Additionally, spectrogram plots for the two separated sources are plotted in Fig. 4(b).

5. Conclusion

In this paper, the S^2H norm is computed. The norm is utilized for clustering based blind source separation in the S^2H-STFT domain. The number of sources is estimated directly from the number of approximated clusters. Noise thresholding is utilized for the steering (mixing) matrix computation. Composite and objective measures are utilized for evaluating the proposed method. The proposed method performs reasonably better than traditional counterparts. The experiments were also carried out on real data. A prototype of S^2MA for BSS applications is currently being explored.

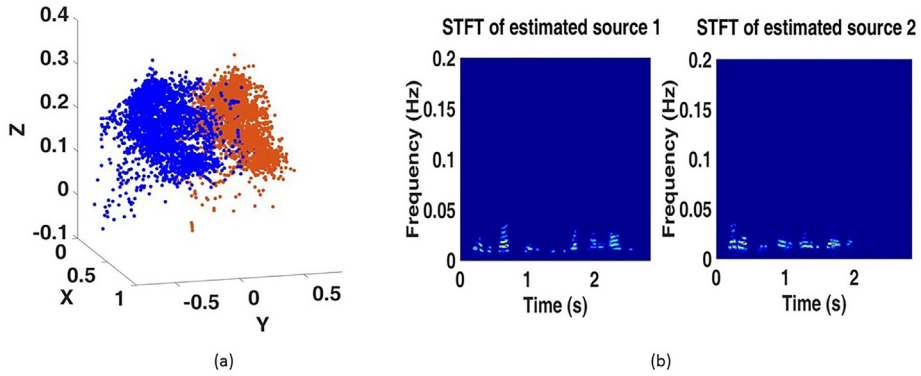

Fig. 4. Illustration of spherical sector harmonics clustering based blind source separation on real data. (a) Two clusters of steering vectors corresponding to two real sources. (b) The STFT plot of the separated sources.

References

[1]P. Dwivedi, G. Routray, and R. M. Hegde, "Spherical harmonics domain-based approach for source localization in presence of directional interference," JASA Express Lett. **2**(11), 114802 (2022).

[2]T. Padois, J. St-Jacques, K. Rouard, N. Quaegebeur, F. Grondin, A. Berry, H. Nelisse, F. Sgard, and O. Doutres, "Acoustic imaging with spherical microphone array and kriging," JASA Express Lett. **3**, 042801 (2023).

[3]N. Epain and C. T. Jin, "Independent component analysis using spherical microphone arrays," Acta Acust. Acust. **98**(1), 91–102 (2012).

[4]Z. Li and R. Duraiswami, "Hemispherical microphone arrays for sound capture and beamforming," in *IEEE Workshop on Applications of Signal Processing to Audio and Acoustics, 2005* (IEEE, Piscataway, NJ, 2005), pp. 106–109.

[5]P. Gautron, J. Krivanek, S. N. Pattanaik, and K. Bouatouch, "A novel hemispherical basis for accurate and efficient rendering," in *EGSR'04: Proceedings of the Fifteenth Eurographics conference on Rendering Techniques* (Eurographics Association, Goslar, Germany, 2004), pp. 321–330.

[6]D. Kumari and L. Kumar, "Acoustic source localization in hemispherical harmonics domain," in *Proceedings of EuroNoise 2018* (European Acoustics Association, 2018), pp. 2575–2580.

[7]P. Lecomte, M. Melon, and L. Simon, "Spherical fraction beamforming," IEEE/ACM Trans. Audio Speech Lang. Process. **28**, 2996–3009 (2020).

[8]D. Kumari and L. Kumar, "Spherical sector harmonics representation of sound fields using a microphone array over spherical sector," J. Acoust. Soc. Am. **149**(1), 145–157 (2021).

[9]D. Kumari and L. Kumar, "S^2H domain processing for acoustic source localization and beamforming using microphone array on spherical sector," IEEE Trans. Sign. Process. **69**, 1983–1994 (2021).

[10]R. Ikeshita and T. Nakatani, "Independent vector extraction for fast joint blind source separation and dereverberation," IEEE Sign. Process. Lett. **28**, 972 (2021).

[11]J. Metsomaa, J. Sarvas, and R. J. Ilmoniemi, "Blind source separation of event-related EEG/MEG," IEEE Trans. Biomed. Eng. **64**(9), 2054–2064 (2017).

[12]S. I. Amari, "Natural gradient works efficiently in learning," Neural Comput. **10**(2), 251–276 (1998).

[13]J.-F. Cardoso, "Blind signal separation: Statistical principles," Proc. IEEE **86**(10), 2009–2025 (1998).

[14]A. Hyvärinen, J. Karhunen, and E. Oja, *Independent Component Analysis* (Wiley, New York, 2004), Vol. 46.

[15]K. Zhang, G. Tian, and T. Lan, "Blind source separation based on JADE algorithm and application," in *3rd International Conference on Mechatronics, Robotics and Automation* (Atlantis Press, Amsterdam, 2015).

[16]A. Aissa-El-Bey, N. Linh-Trung, K. Abed-Meraim, A. Belouchrani, and Y. Grenier, "Underdetermined blind separation of nondisjoint sources in the time-frequency domain," IEEE Trans. Sign. Process. **55**(3), 897–907 (2007).

[17]A. H. Zhang, B. G. Bi, C. S. G. Razul, and D. C. M. See, "Estimation of underdetermined mixing matrix with unknown number of overlapped sources in short-time Fourier transform domain," in *Proceedings of the IEEE International Conference on Acoustics, Speech, and Signal Processing (ICASSP)* (IEEE, Piscataway, NJ, 2013), pp. 6486–6490.

[18]Z. He, L. Yang, J. Liu, Z. Lu, C. He, and Y. Shi, "Blind source separation using clustering-based multivariate density estimation algorithm," IEEE Trans. Sign. Process. **48**(2), 575–579 (2000).

[19]E. Vincent, R. Gribonval, and C. Fevotte, "Performance measurement in blind audio source separation," IEEE Trans. Audio Speech Lang. Process. **14**(4), 1462–1469 (2006).

[20]B. Rafaely, "Analysis and design of spherical microphone arrays," IEEE Trans. Speech Audio Process. **13**(1), 135–143 (2005).

[21]K. Fukunaga and L. Hostetler, "The estimation of the gradient of a density function, with applications in pattern recognition," IEEE Trans. Inf. Theory **21**(1), 32–40 (1975).

[22]*VisiSonics 5/64 Audio Visual Camera*, https://www.visisonics.com/audio-camera (Last viewed 10/4/2023).

[23]J. S. Garofolo, *TIMIT Acoustic-Phonetic Continuous Speech Corpus* (Linguistic Data Consortium, Philadelphia, 1993).

[24]Y. Hu and P. C. Loizou, "Evaluation of objective measures for speech enhancement," in *Ninth International Conference on Spoken Language Processing* (IEEE, Piscataway, NJ, 2006).